The damage signal IL-33 promotes a focal protective myeloid cell response to *Toxoplasma gondii* in the brain

Katherine M. Still*, Samantha J. Batista*, Jeremy A. Thompson*, Nikolas W. Hayes*, Carleigh O'Brien*, and Tajie H. Harris*

Affiliations: *Center for Brain Immunology and Glia, Department of Neuroscience, University of Virginia, Charlottesville, VA 22908

Corresponding Author and Lead Contact:

Tajie H. Harris, MR-4 Room 6148, 409 Lane Road, Charlottesville, VA 22908

Phone: 434-982-6916

Fax: 434-982-4380

Email: tajieharris@virginia.edu

This work was funded by National Institutes of Health grants R01NS091067 to T. H. H., T32GM008328 to K. M. S. and J. A. T., T32AI007046 to S. J. B., and T32AI007496 to C. A. O. and a University of Virginia School of Medicine R&D grant.

SUMMARY

An intact immune response is critical for survival of hosts chronically infected with *Toxoplasma gondii*. We observe clusters of macrophages surrounding replicating parasite in brain tissue, but the initial cues which instruct focal inflammatory reactions in the central nervous system (CNS) are not well understood. One potential mechanism of broad relevance is host cell damage. Here we find that IL-33, a nuclear alarmin, is critical for control of *T. gondii* parasites in the brain. IL-33 is expressed by oligodendrocytes and astrocytes during *T. gondii* infection, and a loss of nuclear IL-33 staining is observed in association with replicating *T. gondii* in infected mouse and human brain tissue, suggestive of IL-33 release. IL-33 signaling is required for induction of chemokines in astrocytes, including focal CCL2 production as visualized using CCL2-mCherry reporter mice. Bone marrow chimera experiments support the hypothesis that IL-33 could be acting directly on astrocytes, as the relevant IL-33-responding cell is radio-resistant. In alignment with CCL2 induction, IL-33 signaling is required for the infiltration of $CCR2^{+}$ myeloid cells that express anti-parasitic iNOS locally. These results expand our knowledge of alarmin signaling in the brain, an environment which is unique from the periphery and demonstrates the importance of a single damage signal in focal control of *T. gondii* infection in the CNS.

38 **INTRODUCTION**

39

40 *Toxoplasma gondii* is a eukaryotic parasite which encysts in the brain parenchyma of its
41 hosts, including humans and mice[1-3]. Mortality from *T. gondii* infection is associated with
42 conversion of the latent cyst form to fast-replicating parasites within CNS tissue. Increased
43 prevalence of parasite replication has been documented in immunosuppressed patients
44 undergoing transplant surgeries[4], HIV-AIDS patients[5-7], and in congenital infection[8]. Murine *T.*
45 *gondii* infection features natural cyst formation with spontaneous reactivation and serves as a
46 model for understanding how protective immune responses are generated in the brain[9,10].

47 A Th1-dominated immune response to *T. gondii* is essential for control of murine
48 infection[1,2]. Depletion of T-cell derived IFN-γ during brain infection results in rapid mortality[11]. IFN-
49 γ can stimulate anti-parasitic effector responses in macrophages, such as the production of
50 reactive nitrogen species[2]. Macrophage-derived inducible nitric oxide synthase (iNOS) is effective
51 at limiting parasite replication via direct toxicity and depletion of arginine *in vitro*[2,12]. iNOS is also
52 vital to survival of chronic brain infection *in vivo*[13,14]. We find that blood-derived iNOS-expressing
53 macrophages form foci around reactivated parasite during chronic infection. But how
54 macrophages are recruited to the brain in response to *T. gondii*, and how they are instructed to
55 reach specific sites within brain tissue where *T. gondii* is replicating is unclear.

56 During the acute, systemic stage of infection, the pattern recognition receptors TLR11 and
57 TLR12 and Nod-like receptors NLRP1 and NLRP3 are involved in the activation of the immune
58 system[15-18], but how and if *T. gondii* is recognized in the brain is not yet characterized. Sensing of
59 damage-associated molecular patterns, however, may be a mechanism of broad relevance by
60 which blood-derived myeloid cells are directed to the brain. Here we focus on a nuclear alarmin,
61 IL-33, which acts as an amplifier of immune responses throughout the body[19-21]. Interestingly, *T.*
62 *gondii*-infected mice deficient for the IL-33 receptor have been reported to exhibit brain pathology

63 and increased parasite burden, but the impact of IL-33 signaling on immune cell recruitment has
64 not been addressed[22].

65 IL-33 is expressed in barrier tissues in the periphery, including the lung, gut, and skin,
66 where it serves as a sentinel for barrier tissue disruption and is best known for its role in promoting
67 type 2 immune responses during asthma, allergy, and helminth infection[19-21,23]. Because this
68 nuclear protein does not contain a secretory signal peptide and does not require processing to be
69 active, it is proposed to be released upon necrotic cell death[19,21,24]. Following its release, IL-33
70 acts on a heterodimer of the IL-1 receptor accessory protein (IL-1RacP) and its cognate receptor
71 ST2 to initiate classical MyD88-NF-κB signaling which upregulates expression of chemokines and
72 cytokines[20,21]. In the periphery, IL-33 can signal on a gamut of ST2-expressing cells of
73 hematopoietic origin; those most commonly studied are type 2 innate lymphoid cells (ILC2s), mast
74 cells, and regulatory T cells[20,21,25]. The ultimate effect of IL-33 signaling depends heavily on the
75 responding cell type and environmental milieu and can serve either an inflammatory or
76 homeostatic function[25].

77 IL-33 is more highly expressed in the brain and spinal cord than any other tissue[23], but its
78 roles are only beginning to be described in the CNS. Nuclear IL-33 is expressed by astrocytes
79 and myelinating oligodendrocytes in the healthy, adult mouse brain parenchyma[26,27]. Like IL-33
80 expression, IL-33 signaling during pathology in the brain likely differs from the periphery. ST2-
81 expressing immune cells are physically separated from IL-33 expressing cells in the parenchyma
82 by the BBB in a naïve state and would likely be unable to respond to initial insult[26,28-31]. Therefore,
83 it is unknown if the generation of an immune response to brain pathology would necessitate IL-
84 33 signaling on a brain-resident cell type. Nonetheless, IL-33 has been recently demonstrated to
85 be beneficial in responding to insults affecting the parenchyma, including mouse models of
86 Alzheimer's disease[32] and stroke[33], in which peripherally-administered IL-33 had beneficial effects
87 on disease outcome. The mechanisms by which endogenous IL-33 generates immunity to various
88 brain insults are still being defined.

89 Here we show that IL-33-expressing glia are lost in regions of replicating parasite within
90 brain tissue. We report that IL-33 signals on a brain-resident responder to recruit blood-derived
91 myeloid cells to the *T. gondii* infected brain. We find IL-33 impacts focal inflammation, inducing
92 localized chemokine expression and iNOS production in macrophages. Although IL-33 has been
93 predominantly connected with type 2 immune responses, we find that IL-33 signaling is required
94 for limiting parasite burden in a heavily Th1-skewed environment. The mechanism outlined here
95 may have relevance to human *T. gondii* infection and other neuropathological models featuring
96 damage of IL-33-expressing glial cells.
97
98

99 **RESULTS**

100

101 **Focal loss of IL-33-expressing glia is associated with replicating *T. gondii* in the**

102 **brain**

103 By four weeks post infection, *T. gondii* traffics to brain tissue of infected mice and exists

104 in an intracellular cyst form which is slow growing[3,34](Figure 1A). Cysts are most prominent in the

105 cerebral cortex[35], but can exist anywhere in the brain[9,36-38], and each cyst can contain hundreds

106 of individual parasites[39]. We observe occasional cyst reactivation in which releases fast-

107 replicating parasites are released into brain tissue (Figure 1A). Clusters of cells surround

108 individual replicating parasites but not *T. gondii* cysts (Figure 1A). Therefore, we hypothesized

109 that local damage signals are released in response to lytic *T. gondii* replication[40] which could

110 mediate cellular recruitment. We focused on one candidate alarmin, IL-33, which is highly

111 expressed in the CNS at baseline[23,26,27]. Consistent with IL-33 being a pre-stored alarmin,

112 expression only mildly increases with infection (Figure S1A). While IL-33 expression is spread

113 evenly throughout the naïve brain[26], we noticed focal loss of nuclear IL-33 staining in association

114 with replicating parasite (Fig. 1B), suggesting potential alarmin release in these regions. In the *T.*

115 *gondii* infected brain parenchyma, IL-33 is expressed by mature, $CC1^+$ mature oligodendrocytes

116 and by astrocytes, the percentage of which varies by brain region (Figures 1C, 1D, 1E, and S1B).

117 In gray matter, such as the cortex, 60% of IL-33 positive cells are oligodendrocytes and the

118 remainder of the IL-33 expression is astrocytic (Figure 1E). But in white matter tracts such as the

119 corpus callosum, nearly all of IL-33-expressing cells are oligodendrocytes (Figures 1D and 1E).

120 Markers for these cell types are also absent at the center of inflammatory lesions, suggestive of

121 glial cell death and possible local release of IL-33 in the *T. gondii*-infected brain parenchyma

122 (Figure S1C).

123 We also detected IL-33 protein expression in astrocytes in healthy human brain tissue, but

124 not in oligodendrocytes (Figures 1F and 1G). Innate recognition of *T. gondii* in the human brain

125 has not been described, due in part to the fact that TLRs 11 and 12 which recognize *T. gondii*
126 acutely in mice are a pseudogene and nonexistent in humans, respectively[2,15,16,41]. In post-mortem
127 brain tissue of a toxoplasmic encephalitis patient, we detected intact IL-33 staining in healthier
128 regions of infected brain tissue, but IL-33 staining was absent from *T. gondii* lesions (Figure S1D).
129 Collectively, these results indicate that IL-33 is expressed by glia in the *T. gondii* infected brain
130 and is absent from lesions where *T. gondii* is replicating.
131
132 **IL-33-ST2 signaling induces localized monocyte chemoattractant, CCL2**

133 In order to interrogate the function of IL-33 in *T. gondii* infection, we considered its
134 described role as an alarmin which recruits and activates immune cells[19-21]. Recruitment of
135 immune cells to the brain is a highly-orchestrated process which requires upregulation of
136 chemokine and adhesion factor expression. We probed whole brain homogenate by qRT-PCR
137 from wildtype and IL-33R(ST2)-deficient mice for discrepancies in genes which could influence
138 immune cell trafficking to the brain. ST2$^{-/-}$ mice exhibited defects in expression of the chemokines
139 *ccl2*, *cxcl10*, and *cxcl1* compared with infected wildtype counterparts (Figure 2A), whereas
140 expression of the adhesion factors *vcam* and *icam* were equivalent between genotypes (Figure
141 2A). Interestingly, *ccl2* and *cxcl10* expression has been attributed to astrocytes by *in situ*
142 hybridization during *T. gondii* infection[42]. Although *cxcl1* has not been extensively studied in our
143 system, it has been reported to be expressed in astrocytes during neuroinflammation[43]. We did
144 not observe an effect, however, of IL-33 signaling on *cxcl9* expression– a chemokine which is
145 made by PU.1-expressing cells, including microglia and macrophages, rather than astrocytes[44]
146 (Fig. 2A). These results suggest that IL-33 may be acting directly on astrocytes to induce
147 chemokine expression during *T. gondii* infection.

148 We next sought to visualize the localization of chemokine expression in relation to parasite
149 replication within brain tissue. We focused on the chemokine with the greatest in expression
150 between WT and ST2$^{-/-}$ mice, the monocyte chemoattractant CCL2. CCL2 expression is highly

151 upregulated in the brain following infection by approximately 100-fold (Fig. S2A). To gain a spatial
152 understanding of CCL2 expression, we infected CCL2-mCherry reporter mice[45] and conducted
153 immunofluorescence microscopy on chronically infected brain tissue. We observed CCL2
154 expression in "hotspots", which were present in brain lesions containing hallmarks of parasite
155 reactivation, including destruction of brain-resident cells, absence of IL-33 staining, and
156 accumulation of immune cells (Figures 2B-2E). Approximately 75% of CCL2-mCherry was
157 expressed by astrocytes and 22% by Iba1^{+} macrophages, and 3% of cells did not co-stain with
158 either of these markers (Figure S2B). CCL2-mCherry signal that could not be attributed to either
159 cell type was present at the center of inflammatory lesions and could be derived from cellular
160 debris or expressed by newly recruited monocytes which do not yet express the macrophage
161 marker Iba1. Expression of CCL2 in inflammatory lesions led us to inquire whether CCL2 could
162 be upregulated locally in response to IL-33. To this end, we crossed CCL2-mCherry reporter mice
163 to ST2$^{-/-}$ mice to visualize CCL2 expression in the absence of IL-33 signaling. Sagittal brain
164 section tile scans revealed that CCL2 foci in ST2$^{-/-}$ mice were much reduced in size compared
165 with wildtype infected mice (Figures 2D and 2E). Multiple signals can likely induce CCL2 during
166 infection, including other innate cytokines[46], but our data suggest that IL-33 is a major contributor
167 to the induction of focal CCL2 expression in the *T. gondii* infected brain (Figures 2D and 2E).
168

169 **Trafficking of blood-derived myeloid cells to the *T. gondii*-infected brain is**
170 **dependent on IL-33-ST2 signaling**

171 We next assessed the impact of IL-33-induced CCL2 expression on the recruitment of
172 myeloid cells to the brain. Specifically, we were interested in the CCR2^{+} monocyte subset and
173 macrophages derived from these cells. To distinguish myeloid cell subsets that enter the brain
174 from the brain-resident microglia, we generated a microglia reporter mouse strain by crossing a
175 CX3CR1-creERT2 mouse to an Ai6 (Zsgreen) cre-reporter mouse. Mice were given tamoxifen at

176 weaning, labeling most myeloid cells, including microglia[47,48]. We waited four weeks post-
177 tamoxifen treatment to allow for peripheral turnover of Zsgreen-expressing cells while microglia
178 remained labeled. With these mice, we were able to visualize a robust increase in cell number of
179 unlabeled (Zsgreen-), $CD45^{hi}$, $CD11b^{+}$ infiltrating myeloid cells in the brain during chronic *T. gondii*
180 infection (Figure 3A). Blood-derived macrophages were not only present in the brain during
181 infection (Figure 3B), but also clustered with high fidelity around replicating parasite (Figure S3A),
182 as distinguished from microglia in brain tissue sections using the microglia reporter mouse. While
183 a small percentage of microglia upregulate CD45 upon infection, we found that over 90% of
184 $Zsgreen^{+}$ microglia were captured by a $CD45^{int}$ gate by flow cytometry (Fig. S3B). Therefore, we
185 used CD45 expression to distinguish microglia from infiltrating myeloid cells in future flow
186 cytometry experiments.

187 Recruitment of myeloid cells to the *T. gondii*-infected brain was dependent on IL-33-ST2
188 signaling. The frequency and number of engrafted myeloid cells denoted by $CD45^{hi}$ $CD11b^{+}$ cells
189 were decreased in infected $ST2^{-/-}$ brains compared with controls by flow cytometry (Figures 3C
190 and 3D), while $CD45^{int}$ $CD11b^{+}$ microglia numbers were unchanged (Figure 3D). Importantly, this
191 phenomenon was brain-specific. $ST2^{-/-}$ spleens contained higher numbers of $CD11b^{+}$ cells than
192 controls, which was not evident at baseline, supportive of a brain recruitment defect (Figures S3C,
193 S3D). Numbers of myeloid cells were also comparable in ST2-deficient and wildtype mice during
194 acute infection (Figure S3E and S3F). To confirm that myeloid cells recruited to the brain were
195 monocyte-derived and capable of responding to CCL2, we crossed $ST2^{-/-}$ mice to a CCR2-RFP
196 reporter mouse. At four weeks post infection, $ST2^{-/-}$ mice displayed a marked decrease in $CCR2^{+}$
197 cell infiltration (Figures 3E, 3F, and 3G) by immunohistochemistry.

198

199 **IL-33 signals on a radio-resistant responder to recruit myeloid cells to the brain**

200 Given that a wide range of cells have been reported to express ST2[19,21,25], we were curious
201 which ST2-expressing cell type was responsible for mediating IL-33-dependent recruitment of

202 myeloid cells to the brain. We detected ST2 on innate lymphoid cells (ILC2s) in the brain, as well
203 as regulatory T cells (Tregs) (Figures S4A and S4B). But it is unclear if ILC2s would be relevant
204 to monocyte recruitment during a Th1-dominated infection, and Tregs are spatially restricted from
205 the parenchyma even after *T. gondii* infection[31]. ST2 mRNA has also been reported in microglia
206 and astrocytes[49]. Therefore, we performed a bone marrow chimera to determine if IL-33 signals
207 on a radio-sensitive or a radio-resistant cell type to recruit myeloid cells to the brain. Briefly, we
208 lethally irradiated wildtype and $ST2^{-/-}$ mice, then reconstituted these mice with bone marrow from
209 wildtype donors or $ST2^{-/-}$ donors, and allowed 6 weeks for reconstitution before infection (Figure
210 3H). We found that ST2-deficient recipients which received wildtype bone marrow resembled
211 ST2-deficient mice which received ST2-deficient bone marrow, suggesting that a hematopoietic
212 source of ST2 is irrelevant for IL-33-mediated recruitment of infiltrating myeloid cells to the brain
213 (Figure 3I). These results are consistent with our hypothesis that IL-33 acts directly on astrocytes
214 to induce CCL2 expression and recruit monocyte-derived myeloid cells to the brain.

215

216 **IL-33-ST2 signaling is required for engrafted myeloid cell-derived iNOS expression**

217

218 We next probed further into the blood-derived myeloid compartment to assess the anti-
219 parasitic capacity of these cells in the absence of IL-33 signaling. One of the most powerful
220 mechanisms myeloid cells can employ to limit parasite is the production of NO by inducible nitric
221 oxide synthase (iNOS)[2,13,14]. We assessed which cells expressed iNOS in the brain by flow
222 cytometry using the microglia reporter mouse. All of the iNOS in the infected brain can be
223 attributed to $CD11b^{+}$ myeloid cells, only a tenth of which is produced by microglia (Figures 4A and
224 4B). Peripherally-derived macrophages far outnumber microglia and the frequency of iNOS
225 expressing cells within the microglia population was also much lower than that of infiltrating
226 myeloid cells (Figure 4A).

227 We found IL-33-ST2 signaling to be required for adequate iNOS expression by
228 peripherally-derived macrophages (Figures 4C and 4D). Beyond a macrophage recruitment

229 defect, iNOS positive infiltrating myeloid cells were reduced in frequency (Figure 4C), suggesting
230 that of the cells that reach the brain, fewer are anti-parasitic without IL-33 signaling. IL-33 is not
231 likely to influence iNOS production in infiltrating macrophages directly, as we did not detect ST2
232 in these cells (Figure S4C). Alternatively, we propose that IL-33-induced chemokine directs
233 infiltrated macrophages to inflammatory lesions where local signals that can upregulate iNOS are
234 concentrated. Indeed, iNOS expression by macrophages in the *T. gondii*-infected brain is
235 localized in clusters, and the size of these foci are dependent on IL-33 signaling (Figures 4E and
236 4F). One signal which is required for iNOS expression is IFN-γ, which acts through STAT1[1,2]. We
237 observe reduced foci of phosphorylated STAT1-positive macrophages in tissue sections in the
238 absence of IL-33 signaling (Figure S4D). These results emphasize that not only are fewer
239 macrophages recruited to the *T. gondii* infected brain in the absence of IL-33 signaling, but fewer
240 are instructed by IFN-γ to make iNOS within inflammatory lesions.
241

242 **ST2$^{-/-}$ mice have deficient CD4^{+} T cell responses**

243 IFN-γ is almost exclusively T cell-derived in the *T. gondii*-infected brain (Figure S5A). Reduced
244 phosphorylated-STAT1 and IFN-γ–inducible iNOS expression in inflammatory foci of infected
245 ST2$^{-/-}$ mice pointed to a reduction in T cell-derived IFN-γ near replicating parasites. T cells are
246 indeed present in lesions containing replicating *T. gondii*, but cluster less densely than
247 macrophages (Figure S5B). When we assessed T cell numbers by flow cytometry in ST2 deficient
248 mice, we observed a decrease in CD4^{+}, but not CD8^{+} T cells (Figure 5A). CD4^{+} T cells displayed
249 reduced proliferation, *T. gondii*-tetramer specificity, and cytokine secretion in ST2$^{-/-}$ mice (Figures
250 5B and 5C), whereas CD8^{+} function was unaffected (Figures S5C and S5D). These results could
251 potentially be explained by the decrease of MHCII-expressing cells in the brains of ST2$^{-/-}$ mice,
252 which may provide less opportunity for local CD4^{+} T cell activation (Figure 5D). Importantly, T cell
253 responses were unaffected in the periphery and during the acute stage of infection in ST2$^{-/-}$ mice

254 (Figures S5E-G). These results highlight the compounding effect of ST2 deficiency in anti-
255 parasitic capacity displayed by both myeloid cells and T cells during chronic *T. gondii* infection.
256
257 **IL-33-ST2 signaling is required for control of brain parasite burden**
258
259 The ultimate consequence of the absence of IL-33-ST2 signaling is an increase in brain
260 parasite burden (Figures 6A, 6B). Tissue cysts observed by H & E staining of infected brain tissue
261 were present in clusters in ST2$^{-/-}$ mice, a phenomenon which does not occur frequently in wildtype
262 mice (Figure 6A). We propose that in ST2$^{-/-}$ mice, parasite reactivation events are not properly
263 controlled, resulting in increased opportunity for parasite to encyst in neighboring cells.
264 Importantly, parasite was cleared from peripheral tissues in acute stages of infection in ST2-
265 deficient mice (data not shown). While parasite burden does increase, ST2$^{-/-}$ mice do not succumb
266 to infection, which implies that there are additional signals that mobilize and shape the protective
267 immune response to chronic *Toxoplasma gondii* infection. In any case, IL-33 plays a non-
268 redundant role and contributes significantly to the control of chronic *T. gondii* infection.
269
270

DISCUSSION

Instructing immune cells to enter the brain and reach particular sites within brain tissue requires fine-tuned orchestration[50-52]. Chemokines can impact behavior and interaction of immune cells within the brain parenchyma[52], but the signals which precede chemokine production, in our system and in many others, are often not understood. Our results pinpoint a damage-associated cue, IL-33, which induces localized production of monocyte chemoattractant in the *T. gondii*-infected brain. IL-33 is necessary for the congregation of nitric-oxide-producing myeloid cells within the parenchyma and, consequently, is necessary to limit parasite burden.

There are several interesting aspects of IL-33 expression which lend themselves to further study. Each tissue in the body contains resident cells that detect perturbations and communicate to peripheral immune cells[53]. In both the naïve and *T. gondii*-infected adult brain parenchyma, IL-33 is not expressed by all brain-resident cells, but rather is restricted to myelinating oligodendrocytes and astrocytes. This is in stark contrast to HMGB1, which is expressed ubiquitously in the brain[30]. Common intracellular contents which can also signal damage, such as ATP and uric acid, are also housed in nearly all cell types. We find that the majority of IL-33 expression in the infected, adult mouse brain is derived from oligodendrocytes, specifically, mature myelinating oligodendrocytes, implicating these cells as sentinels of tissue damage. IL-33 expression by mature oligodendrocytes, rather than oligodendrocyte progenitors is consistent with the observation of IL-33 expression in terminally differentiated cells throughout the rest of the body, including barrier cells and cardiomyocytes[20,54,55]. Oligodendrocytes are uniquely susceptible to several initiators of cell death, including oxidative stress, sphingolipid-derived ceramide signaling, and glutamate excitotoxicity[56]. IL-33 may be involved in any brain insult associated with oligodendrocyte death, including even normal aging, where excitotoxicity to oligodendrocytes has been reported[56,57].

We have identified IL-33 expression by astrocytes in the healthy human brain, but not by oligodendrocytes. Discrepancies by which brain cells release IL-33 between humans and mice is

298 of translational interest and is a topic for further study. We posit that IL-33 signaling has relevance
299 to human *T. gondii* infection, as we documented a loss of IL-33 staining in regions of parasite
300 deposition within the brain of a human toxoplasmic encephalitis patient. Recognition of damage
301 caused by a pathogen may be a more broadly relevant mechanism for engendering an immune
302 response than recognition of the pathogen itself through germline encoded receptors. Alarmin
303 signaling would allow more species, including humans, to detect *Toxoplasma*, since the murine-
304 specific TLRs 11 and 12 which recognize a *T. gondii* cytoskeletal protein are a pseudogene or
305 nonexistent in humans, respectively[15,16,41,58,59]. IL-33 signaling could result in similar
306 consequences as TLR signaling described in response to *T. gondii* in mice, since both pathways
307 converge on MyD88 and NF-κB[30].

308 We have established that IL-33 acts on a radio-resistant responder to recruit immune cells
309 to the *T. gondii*-infected brain, although IL-33 has been most commonly reported to signal on
310 immune cells in the periphery[19-21,25]. For reasons that are unclear, ST2 expression has not been
311 convincingly shown on the protein level on any brain resident cell types, but IL-33 ST2 signaling
312 on glia has been suggested in other studies focused on the CNS. In the retina, IL-33 is released
313 from, and acts on, Müller cells in an autocrine fashion in response to phototoxic stress[55]. In the
314 brain, ST2 mRNA has been detected in both astrocytes and microglia[49]. During brain
315 development, specific deletion of ST2 in microglia led to disrupted synapse engulfment[27]. There
316 is also a suggestion that the relevant ST2-bearing cell can rapidly change with insult. A prior study
317 demonstrated that a $CD11b^+$ fraction from uninjured spinal cord was ST2 positive, whereas the
318 majority of ST2 expression from contused spinal cord glia was CD11b-negative[26]. Indeed, we
319 observe by RNA-seq that microglia express detectable ST2 at baseline, but expression decreases
320 10-fold with infection (unpublished observations). The current study implicates astrocytes as a
321 potential responder to IL-33 during infection. Therefore, our study and others support a glia-glia
322 communication for IL-33 signaling in the CNS.

323 The most well-described function of IL-33 is the potentiation of type 2 immune responses,
324 characterized by secretion of the cytokines IL-4, IL-5, and IL-13, and the involvement of type 2
325 innate lymphoid cells and alternatively activated macrophages[19-21,25]. But the definition of IL-33
326 signaling is broadening; IL-33 now has described roles for inducing a Th1-skewed immune
327 response[60,61], and roles in tissue homeostasis[25]. Our work furthers the idea that the outcome of
328 IL-33 signaling is highly dependent on the inflammatory environment. We find that IL-33 plays a
329 role in potentiating the type 1-skewed response necessary for controlling *T. gondii* in the brain.
330 We demonstrate that IL-33 is required for myeloid cell-derived nitric oxide production in
331 inflammatory lesions. It is unclear how IL-33 mediates this effect, since iNOS-positive cells in our
332 system do not express ST2. We suggest that IL-33 recruits cells via astrocyte-derived chemokine
333 to areas in the brain which contain signals to induce iNOS expression. One of these is likely IFN-
334 γ, but it is possible that other alarmins, or recognition of the parasite itself, could influence anti-
335 parasitic capacity in inflammatory lesions. IL-33 signaling also did not seem to impact the brain
336 vasculature, but other alarmins may activate the vasculature to promote monocyte cell entry,
337 illustrating the complex process necessary for recruitment of cells to specific regions of the CNS.
338 Ultimately, our results demonstrate the importance of one alarmin in controlling a
339 pathogen which infects the brain parenchyma. IL-33 signaling is required for local immune
340 responses generated during *T. gondii* infection of the immunologically-unique CNS. Since ST2$^{-/-}$
341 mice do not succumb to infection, additional mechanisms are likely at play during chronic *T. gondii*
342 infection, including signaling by other alarmins, such as ATP, HMGB1, S100 proteins, and IL-1α.
343
344
345
346

ACKNOWLEDGEMENTS

The authors would like to acknowledge members of the Harris lab and center for Brain Immunology and Glia (BIG) for their valuable input during the development of this work. We thank Sachin P. Gadani and Kenneth S. Tung for the discussions regarding IL-33. We thank Marieke K. Jones for her guidance with statistical analysis and coding. We would like to acknowledge the support we received from core facilities at the University of Virginia, including the Biorepository and Tissue Research Facility, the Flow Cytometry Core, and the Research Histology Core.

CONTRIBUTIONS

Conceptualization, K. M. S. and T. H. H.; Investigation, K. M. S., S. J. B., J. A. T., N. W. H., and C. A. O.; Writing—Original Draft, K. M. S.; Writing—Reviewing and Editing, K. M. S., S. J. B., N. W. H., C. A. O., and T. H. H.; Funding Acquisition, T. H. H.; Supervision, T. H. H.

DECLARATION OF INTERESTS

The authors declare no competing interests.

362 **REFERENCES**

363 1 Hunter, C. A. & Sibley, L. D. Modulation of innate immunity by Toxoplasma gondii virulence
364 effectors. *Nat Rev Microbiol* **10**, 766-778, doi:10.1038/nrmicro2858 (2012).
365 2 Yarovinsky, F. Innate immunity to Toxoplasma gondii infection. *Nat Rev Immunol* **14**, 109-
366 121, doi:10.1038/nri3598 (2014).
367 3 Dubey, J. P., Lindsay, D. S. & Speer, C. A. Structures of Toxoplasma gondii tachyzoites,
368 bradyzoites, and sporozoites and biology and development of tissue cysts. *Clin Microbiol*
369 *Rev* **11**, 267-299 (1998).
370 4 Slavin, M. A., Meyers, J. D., Remington, J. S. & Hackman, R. C. Toxoplasma gondii
371 infection in marrow transplant recipients: a 20 year experience. *Bone Marrow Transplant*
372 **13**, 549-557 (1994).
373 5 Luft, B. J. & Remington, J. S. Toxoplasmic encephalitis in AIDS. *Clin Infect Dis* **15**, 211-
374 222 (1992).
375 6 Luft, B. J. & Remington, J. S. AIDS commentary. Toxoplasmic encephalitis. *J Infect Dis*
376 **157**, 1-6 (1988).
377 7 Hunter, C. A. & Remington, J. S. Immunopathogenesis of toxoplasmic encephalitis. *J*
378 *Infect Dis* **170**, 1057-1067 (1994).
379 8 Frenkel, J. K. Congenital toxoplasmosis: prevention or palliation? *Am J Obstet Gynecol*
380 **141**, 359-361 (1981).
381 9 Ferguson, D. J., Graham, D. I. & Hutchison, W. M. Pathological changes in the brains of
382 mice infected with Toxoplasma gondii: a histological, immunocytochemical and
383 ultrastructural study. *Int J Exp Pathol* **72**, 463-474 (1991).
384 10 Waree, P., Ferguson, D. J., Pongponratn, E., Chaisri, U. & Sukthana, Y.
385 Immunohistochemical study of acute and chronic toxoplasmosis in experimentally infected
386 mice. *Southeast Asian J Trop Med Public Health* **38**, 223-231 (2007).
387 11 Gazzinelli, R., Xu, Y., Hieny, S., Cheever, A. & Sher, A. Simultaneous depletion of CD4+
388 and CD8+ T lymphocytes is required to reactivate chronic infection with Toxoplasma
389 gondii. *J Immunol* **149**, 175-180 (1992).
390 12 Fox, B. A., Gigley, J. P. & Bzik, D. J. Toxoplasma gondii lacks the enzymes required for
391 de novo arginine biosynthesis and arginine starvation triggers cyst formation. *Int J*
392 *Parasitol* **34**, 323-331, doi:10.1016/j.ijpara.2003.12.001 (2004).
393 13 Scharton-Kersten, T. M., Yap, G., Magram, J. & Sher, A. Inducible nitric oxide is essential
394 for host control of persistent but not acute infection with the intracellular pathogen
395 Toxoplasma gondii. *J Exp Med* **185**, 1261-1273 (1997).
396 14 Schluter, D. *et al.* Inhibition of inducible nitric oxide synthase exacerbates chronic cerebral
397 toxoplasmosis in Toxoplasma gondii-susceptible C57BL/6 mice but does not reactivate
398 the latent disease in T. gondii-resistant BALB/c mice. *J Immunol* **162**, 3512-3518 (1999).
399 15 Yarovinsky, F. *et al.* TLR11 activation of dendritic cells by a protozoan profilin-like protein.
400 *Science* **308**, 1626-1629, doi:10.1126/science.1109893 (2005).
401 16 Koblansky, A. A. *et al.* Recognition of profilin by Toll-like receptor 12 is critical for host
402 resistance to Toxoplasma gondii. *Immunity* **38**, 119-130,
403 doi:10.1016/j.immuni.2012.09.016 (2013).
404 17 Gorfu, G. *et al.* Dual role for inflammasome sensors NLRP1 and NLRP3 in murine
405 resistance to Toxoplasma gondii. *MBio* **5**, doi:10.1128/mBio.01117-13 (2014).
406 18 Ewald, S. E., Chavarria-Smith, J. & Boothroyd, J. C. NLRP1 is an inflammasome sensor
407 for Toxoplasma gondii. *Infect Immun* **82**, 460-468, doi:10.1128/IAI.01170-13 (2014).
408 19 Martin, N. T. & Martin, M. U. Interleukin 33 is a guardian of barriers and a local alarmin.
409 *Nat Immunol* **17**, 122-131, doi:10.1038/ni.3370 (2016).
410 20 Liew, F. Y., Girard, J. P. & Turnquist, H. R. Interleukin-33 in health and disease. *Nat Rev*
411 *Immunol* **16**, 676-689, doi:10.1038/nri.2016.95 (2016).

21 Liew, F. Y., Pitman, N. I. & McInnes, I. B. Disease-associated functions of IL-33: the new kid in the IL-1 family. *Nat Rev Immunol* **10**, 103-110, doi:10.1038/nri2692 (2010).
22 Jones, L. A. *et al.* IL-33 receptor (T1/ST2) signalling is necessary to prevent the development of encephalitis in mice infected with Toxoplasma gondii. *Eur J Immunol* **40**, 426-436, doi:10.1002/eji.200939705 (2010).
23 Schmitz, J. *et al.* IL-33, an interleukin-1-like cytokine that signals via the IL-1 receptor-related protein ST2 and induces T helper type 2-associated cytokines. *Immunity* **23**, 479-490, doi:10.1016/j.immuni.2005.09.015 (2005).
24 Cayrol, C. & Girard, J. P. The IL-1-like cytokine IL-33 is inactivated after maturation by caspase-1. *Proc Natl Acad Sci U S A* **106**, 9021-9026, doi:10.1073/pnas.0812690106 (2009).
25 Molofsky, A. B., Savage, A. K. & Locksley, R. M. Interleukin-33 in Tissue Homeostasis, Injury, and Inflammation. *Immunity* **42**, 1005-1019, doi:10.1016/j.immuni.2015.06.006 (2015).
26 Gadani, S. P., Walsh, J. T., Smirnov, I., Zheng, J. & Kipnis, J. The glia-derived alarmin IL-33 orchestrates the immune response and promotes recovery following CNS injury. *Neuron* **85**, 703-709, doi:10.1016/j.neuron.2015.01.013 (2015).
27 Vainchtein, I. D. *et al.* Astrocyte-derived interleukin-33 promotes microglial synapse engulfment and neural circuit development. *Science* **359**, 1269-1273, doi:10.1126/science.aal3589 (2018).
28 Louveau, A., Harris, T. H. & Kipnis, J. Revisiting the Mechanisms of CNS Immune Privilege. *Trends Immunol* **36**, 569-577, doi:10.1016/j.it.2015.08.006 (2015).
29 Gadani, S. P., Smirnov, I., Smith, A. T., Overall, C. C. & Kipnis, J. Characterization of meningeal type 2 innate lymphocytes and their response to CNS injury. *J Exp Med* **214**, 285-296, doi:10.1084/jem.20161982 (2017).
30 Gadani, S. P., Walsh, J. T., Lukens, J. R. & Kipnis, J. Dealing with Danger in the CNS: The Response of the Immune System to Injury. *Neuron* **87**, 47-62, doi:10.1016/j.neuron.2015.05.019 (2015).
31 O'Brien, C. A. *et al.* CD11c-Expressing Cells Affect Regulatory T Cell Behavior in the Meninges during Central Nervous System Infection. *J Immunol* **198**, 4054-4061, doi:10.4049/jimmunol.1601581 (2017).
32 Fu, A. K. *et al.* IL-33 ameliorates Alzheimer's disease-like pathology and cognitive decline. *Proc Natl Acad Sci U S A* **113**, E2705-2713, doi:10.1073/pnas.1604032113 (2016).
33 Luo, H., Higuchi, K., Matsumoto, K. & Mori, M. An interleukin-33 gene polymorphism is a modifier for eosinophilia in rats. *Genes Immun* **14**, 192-197, doi:10.1038/gene.2013.7 (2013).
34 Saeij, J. P., Boyle, J. P., Grigg, M. E., Arrizabalaga, G. & Boothroyd, J. C. Bioluminescence imaging of Toxoplasma gondii infection in living mice reveals dramatic differences between strains. *Infect Immun* **73**, 695-702, doi:10.1128/IAI.73.2.695-702.2005 (2005).
35 Cabral, C. M. *et al.* Neurons are the Primary Target Cell for the Brain-Tropic Intracellular Parasite Toxoplasma gondii. *PLoS Pathog* **12**, e1005447, doi:10.1371/journal.ppat.1005447 (2016).
36 Di Cristina, M. *et al.* Temporal and spatial distribution of Toxoplasma gondii differentiation into Bradyzoites and tissue cyst formation in vivo. *Infect Immun* **76**, 3491-3501, doi:10.1128/IAI.00254-08 (2008).
37 Kittas, S., Kittas, C., Paizi-Biza, P. & Henry, L. A histological and immunohistochemical study of the changes induced in the brains of white mice by infection with Toxoplasma gondii. *Br J Exp Pathol* **65**, 67-74 (1984).
38 Berenreiterova, M., Flegr, J., Kubena, A. A. & Nemec, P. The distribution of Toxoplasma gondii cysts in the brain of a mouse with latent toxoplasmosis: implications for the

behavioral manipulation hypothesis. *PLoS One* **6**, e28925, doi:10.1371/journal.pone.0028925 (2011).

39 Hill, D. E., Chirukandoth, S. & Dubey, J. P. Biology and epidemiology of Toxoplasma gondii in man and animals. *Anim Health Res Rev* **6**, 41-61 (2005).

40 Black, M. W. & Boothroyd, J. C. Lytic cycle of Toxoplasma gondii. *Microbiol Mol Biol Rev* **64**, 607-623 (2000).

41 Roach, J. C. *et al.* The evolution of vertebrate Toll-like receptors. *Proc Natl Acad Sci U S A* **102**, 9577-9582, doi:10.1073/pnas.0502272102 (2005).

42 Strack, A., Asensio, V. C., Campbell, I. L., Schluter, D. & Deckert, M. Chemokines are differentially expressed by astrocytes, microglia and inflammatory leukocytes in Toxoplasma encephalitis and critically regulated by interferon-gamma. *Acta Neuropathol* **103**, 458-468, doi:10.1007/s00401-001-0491-7 (2002).

43 Kang, Z. *et al.* Act1 mediates IL-17-induced EAE pathogenesis selectively in NG2+ glial cells. *Nat Neurosci* **16**, 1401-1408, doi:10.1038/nn.3505 (2013).

44 Ellis, S. L. *et al.* The cell-specific induction of CXC chemokine ligand 9 mediated by IFN-gamma in microglia of the central nervous system is determined by the myeloid transcription factor PU.1. *J Immunol* **185**, 1864-1877, doi:10.4049/jimmunol.1000900 (2010).

45 Shi, C. *et al.* Bone marrow mesenchymal stem and progenitor cells induce monocyte emigration in response to circulating toll-like receptor ligands. *Immunity* **34**, 590-601, doi:10.1016/j.immuni.2011.02.016 (2011).

46 Shi, C. & Pamer, E. G. Monocyte recruitment during infection and inflammation. *Nat Rev Immunol* **11**, 762-774, doi:10.1038/nri3070 (2011).

47 Yona, S. *et al.* Fate mapping reveals origins and dynamics of monocytes and tissue macrophages under homeostasis. *Immunity* **38**, 79-91, doi:10.1016/j.immuni.2012.12.001 (2013).

48 Madisen, L. *et al.* A robust and high-throughput Cre reporting and characterization system for the whole mouse brain. *Nat Neurosci* **13**, 133-140, doi:10.1038/nn.2467 (2010).

49 Yasuoka, S. *et al.* Production and functions of IL-33 in the central nervous system. *Brain Res* **1385**, 8-17, doi:10.1016/j.brainres.2011.02.045 (2011).

50 Sa, Q. *et al.* VCAM-1/alpha4beta1 integrin interaction is crucial for prompt recruitment of immune T cells into the brain during the early stage of reactivation of chronic infection with Toxoplasma gondii to prevent toxoplasmic encephalitis. *Infect Immun* **82**, 2826-2839, doi:10.1128/IAI.01494-13 (2014).

51 Wilson, E. H., Weninger, W. & Hunter, C. A. Trafficking of immune cells in the central nervous system. *J Clin Invest* **120**, 1368-1379, doi:10.1172/JCI41911 (2010).

52 Harris, T. H. *et al.* Generalized Levy walks and the role of chemokines in migration of effector CD8+ T cells. *Nature* **486**, 545-548, doi:10.1038/nature11098 (2012).

53 von Moltke, J. & Pepper, M. Sentinels of the Type 2 Immune Response. *Trends Immunol* **39**, 99-111, doi:10.1016/j.it.2017.10.004 (2018).

54 Chen, W. Y., Hong, J., Gannon, J., Kakkar, R. & Lee, R. T. Myocardial pressure overload induces systemic inflammation through endothelial cell IL-33. *Proc Natl Acad Sci U S A* **112**, 7249-7254, doi:10.1073/pnas.1424236112 (2015).

55 Xi, H. *et al.* IL-33 amplifies an innate immune response in the degenerating retina. *J Exp Med* **213**, 189-207, doi:10.1084/jem.20150894 (2016).

56 McTigue, D. M. & Tripathi, R. B. The life, death, and replacement of oligodendrocytes in the adult CNS. *J Neurochem* **107**, 1-19, doi:10.1111/j.1471-4159.2008.05570.x (2008).

57 Mattson, M. P. Excitotoxic and excitoprotective mechanisms: abundant targets for the prevention and treatment of neurodegenerative disorders. *Neuromolecular Med* **3**, 65-94, doi:10.1385/NMM:3:2:65 (2003).

512 58 Andrade, W. A. *et al.* Combined action of nucleic acid-sensing Toll-like receptors and
513 TLR11/TLR12 heterodimers imparts resistance to Toxoplasma gondii in mice. *Cell Host*
514 *Microbe* **13**, 42-53, doi:10.1016/j.chom.2012.12.003 (2013).
515 59 Gazzinelli, R. T., Mendonca-Neto, R., Lilue, J., Howard, J. & Sher, A. Innate resistance
516 against Toxoplasma gondii: an evolutionary tale of mice, cats, and men. *Cell Host Microbe*
517 **15**, 132-138, doi:10.1016/j.chom.2014.01.004 (2014).
518 60 Baumann, C. *et al.* T-bet- and STAT4-dependent IL-33 receptor expression directly
519 promotes antiviral Th1 cell responses. *Proc Natl Acad Sci U S A* **112**, 4056-4061,
520 doi:10.1073/pnas.1418549112 (2015).
521 61 Bonilla, W. V. *et al.* The alarmin interleukin-33 drives protective antiviral CD8(+) T cell
522 responses. *Science* **335**, 984-989, doi:10.1126/science.1215418 (2012).
523

524

525 **FIGURES**

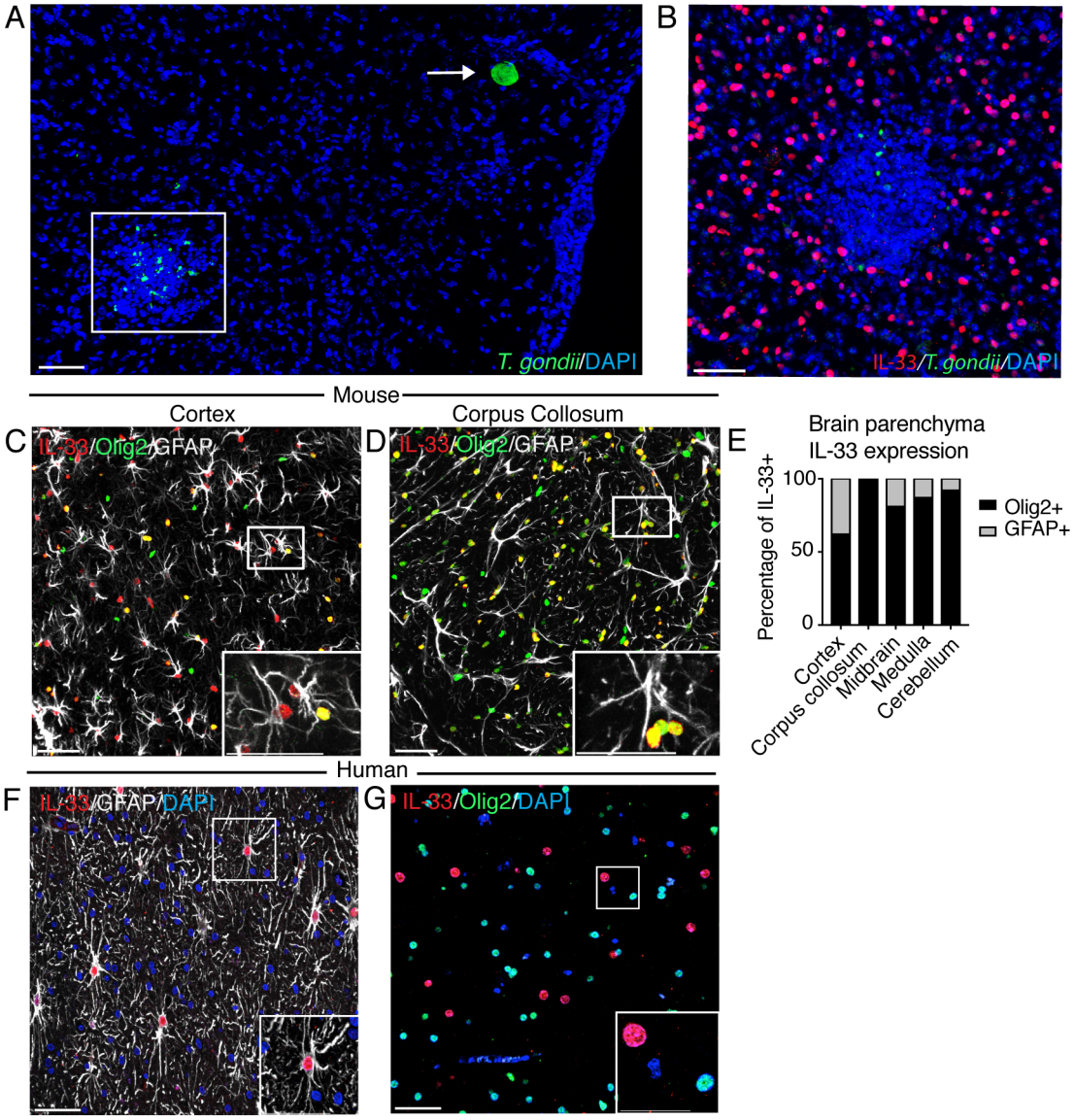

526

527 **Figure 1. Focal loss of IL-33 is associated with replicating *T. gondii* in the brain**

528 (A) Immunofluorescence staining of chronically infected mouse cortex for *T. gondii* (green) -

529 detected in cyst form (arrow) and its reactivated replicating form (box), DAPI staining was used

530 to detect nuclei (blue)

531 (B) Immunofluorescence staining of an inflammatory lesion for IL-33 (red) and *T. gondii* (green)

532 in chronically infected mouse brain tissue – DAPI staining was used to detect nuclei (blue)

533 (C-D) Representative brain region immunofluorescence staining for IL-33 (red), Olig2$^+$
534 oligodendrocytes (green), and GFAP$^+$ astrocytes (white) in chronically infected mouse gray matter
535 (cortex) (C) and white matter (corpus collosum) (D)
536 (E) Percentage of IL-33$^+$ cells which are Olig2$^+$ oligodendrocytes or GFAP$^+$ astrocytes by brain
537 region, n=>30 cells per brain region, representative of 2 independent experiments
538 (F-G) Immunofluorescence staining of healthy human temporal lobe brain tissue for IL-33 (red),
539 colocalized with GFAP$^+$ astrocytes (white) (F), and not co-localized with Olig2$^+$ oligodendrocytes
540 (green) (G), (n=3), scale bars = 50μm
541 See also Figure S1

542
543

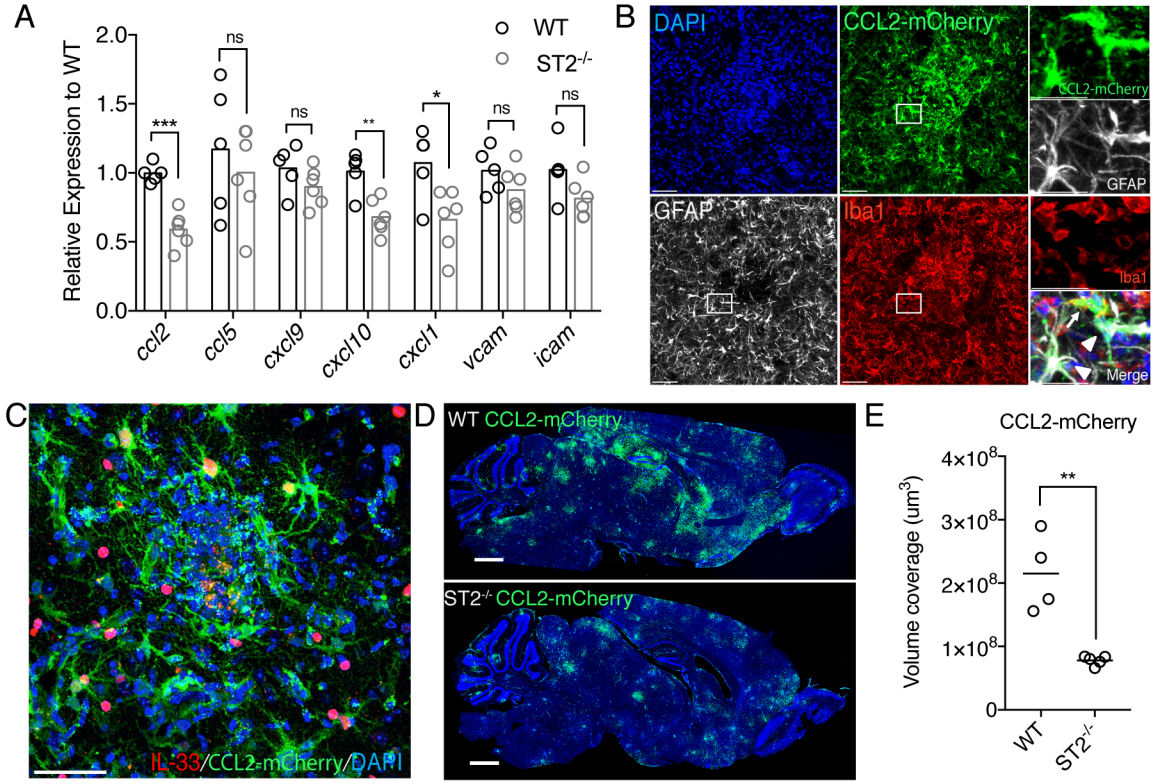

544

545 **Figure 2. IL-33-ST2 signaling induces localized monocyte chemoattractant, CCL2**

546 (A) Quantitative real time PCR was performed on RNA isolated from whole brain homogenate of

547 chronically infected wildtype and ST2$^{-/-}$ mice, (n=5-6 per group, Student's t-test)

548 (B) Immunofluorescence staining of an inflammatory lesion in chronically infected CCL2-mCherry

549 reporter brain tissue for mCherry (green), GFAP^{+} astrocytes (white), and Iba1^{+} macrophages (red)

550 – DAPI staining was used to detect nuclei (blue), scale bar = 50μm. Insets depict co-stained

551 CCL2-mCherry with GFAP^{+} astrocytes and an Iba1^{+} macrophage, scale bar = 20μm

552 (C) Immunofluorescence staining of an inflammatory lesion in chronically infected mouse brain

553 tissue for IL-33 (red) and mCherry (green) – DAPI was used to detect nuclei (blue), scale bar =

554 50μm

555 (D) Representative tile scans of chronically infected wildtype and ST2$^{-/-}$ CCL2-mCherry reporter
556 mice. Sagittal brain slices were stained for mCherry and DAPI staining was used to detect nuclei
557 (blue), scale bar = 2000 µm
558 (E) Quantification of (D) by volume coverage of CCL2-mCherry voxels in sagittal brain sections
559 using Imaris software, (n=4-5 per group, Student's t-test, data points are representative of 3
560 averaged brain sections per mouse, overall data is representative of 3 independent experiments)
561 ns=p>0.05, *=p<0.05, **=p<0.01, ***=p<0.001
562 See also Figure S2.
563
564
565

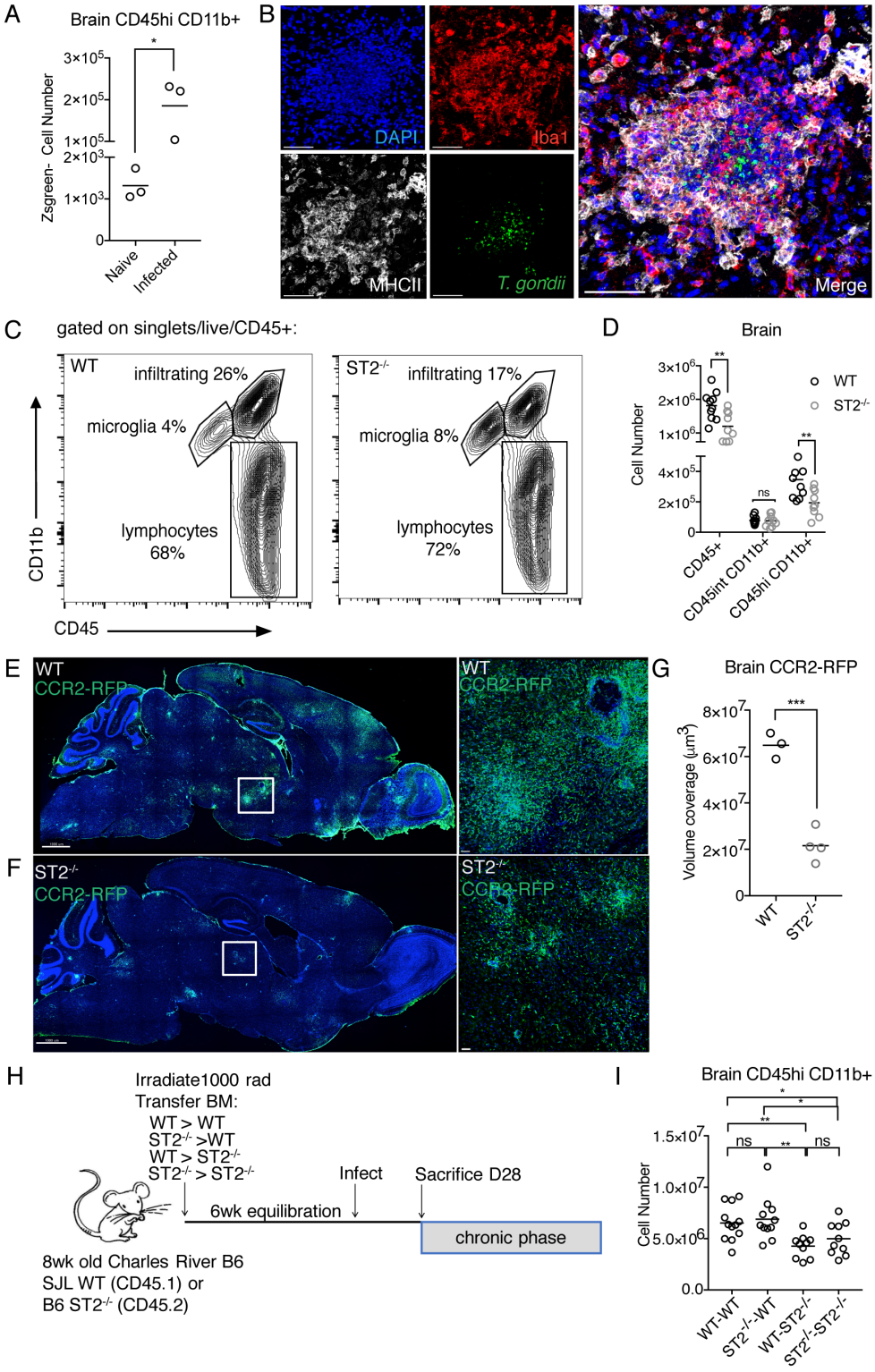

Figure 3. Trafficking of blood-derived myeloid cells to the *T. gondii*-infected brain is dependent on ST2 signaling on a radio-resistant responder

569 (A) Flow cytometry staining of brain mononuclear cells from naïve and chronically infected
570 CX3CR1creERT2 Zsgreen microglia reporter mice. Zsgreen^{-} CD45^{hi}, CD11b^{+} (infiltrating myeloid)
571 cell number was measured before and after infection, (n=3, Student's t-test, representative of 2
572 independent experiments)
573 (B) Immunofluorescence staining of an inflammatory focus in chronically infected wildtype mouse
574 brain tissue for Iba1^{+} macrophages (red), MHCII^{+} cells (white), and *T. gondii* (green) – DAPI was
575 used to detect nuclei (blue), scale bar = 50μm
576 (C) Representative flow cytometry plots measuring CD45 and CD11b expression in chronically
577 infected wildtype and ST2$^{-/-}$ brains
578 (D) Flow cytometry measurement of total CD45^{+} immune cell number, CD45^{int} CD11b^{+} microglia
579 number, and CD45^{hi} CD11b^{+} infiltrating myeloid number in chronically infected WT and ST2$^{-/-}$
580 brains, (n=3-4 per group, data was pooled from 3 experiments and analyzed by randomized block
581 ANOVA).
582 (E-F) Representative tile scans of chronically infected wildtype and ST2$^{-/-}$ CCR2-RFP reporter
583 mice. Sagittal brain slices were stained for RFP and DAPI staining was used to detect nuclei
584 (blue), scale bar = 2000 μm, inset scale bar = 50μm
585 (G) Quantification of (E and F) by volume coverage of CCR2-RFP in sagittal brain sections using
586 Imaris software, (n=3-4 per group, Student's t-test. Data points are representative of 3 averaged
587 brain sections per mouse, performed once)
588 (H) Bone marrow chimera schematic – wildtype and ST2$^{-/-}$ mice were lethally irradiated and
589 reconstituted with either wildtype or ST2$^{-/-}$ bone marrow. Mice were given six weeks for bone
590 marrow to reconstitute prior to infection. Mice were sacrificed at 28 dpi and infiltrating myeloid cell
591 numbers were assessed by flow cytometry.
592 (I) Flow cytometry measurement of CD45^{hi} CD11b^{+} infiltrating myeloid number in chronically
593 infected chimera groups (n=5-6 per group, data was pooled from 2 experiments to demonstrate
594 variability by infection and analyzed by randomized block ANOVA)

595 ns=p>0.05, *=p<0.05, **=p<0.01, ***=p<0.001

596 See also Figure S3.

597

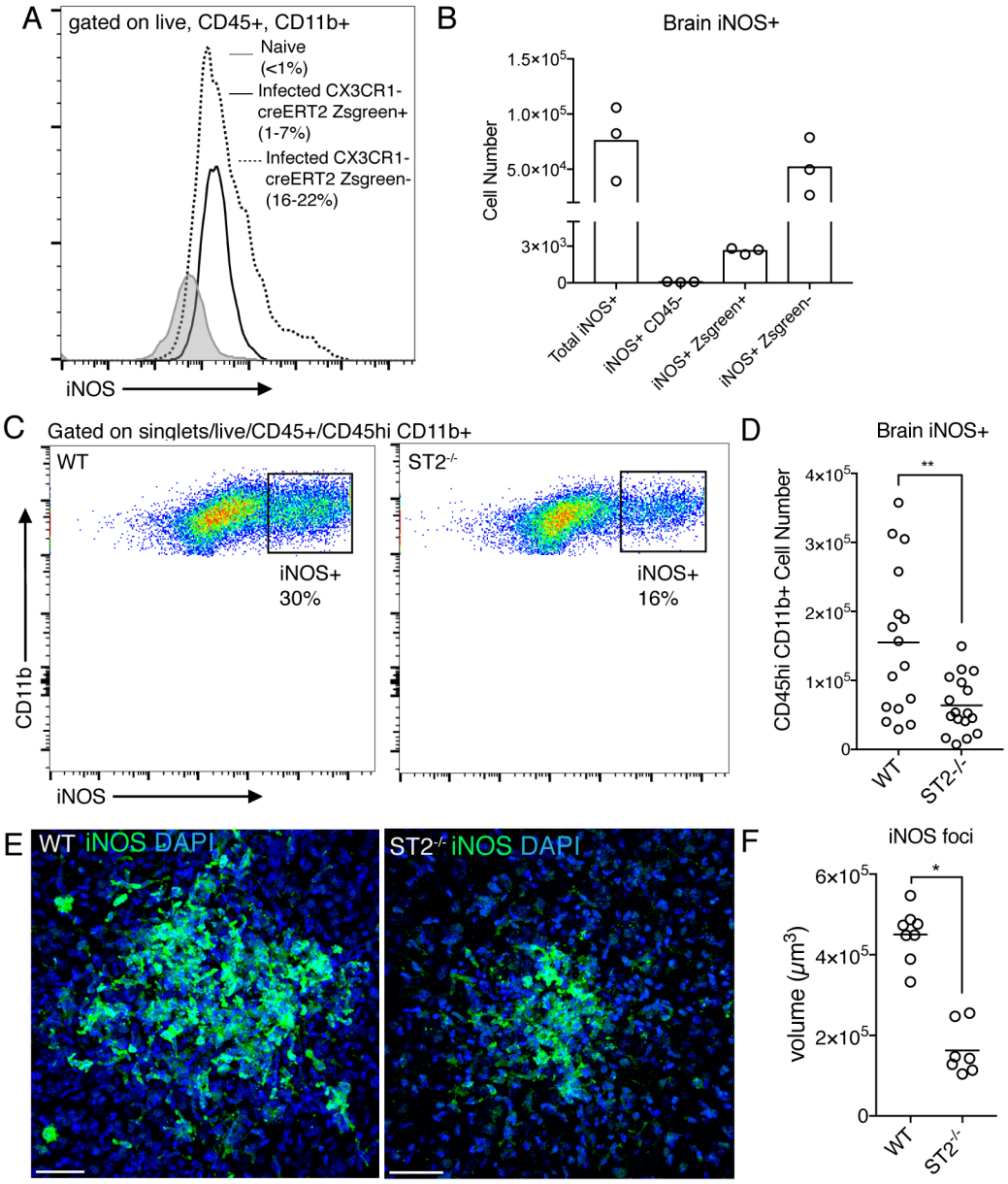

598

599 **Figure 4. IL-33-ST2 signaling is required for engrafted myeloid cell-derived iNOS**

600 (A) Representative flow cytometry histogram demonstrating iNOS expression in naïve and

601 chronically infected CX3CR1-creERT2 ZsGreen microglia reporter mice. Microglia are ZsGreen^{+}

602 and brain-infiltrating CD45^{hi} CD11b^{+} cells are ZsGreen-negative. (n=3, representative of 2

603 independent experiments)

604 (B) Flow cytometry measurement of iNOS^{+} cells in brains of chronically infected CX3CR1-
605 creERT2 ZsGreen microglia reporter mice. ZsGreen- cells are CD45^{hi} CD11b^{+} myeloid cells. (n=3,
606 representative of 2 independent experiments).
607 (C) Representative flow cytometry dot plots measuring iNOS^{+} frequency of CD45^{hi} CD11b^{+} brain-
608 infiltrating cells in chronically infected wildtype and ST2$^{-/-}$ mice
609 (D) Flow cytometry measurement of brain infiltrating CD45^{hi} CD11b^{+} iNOS^{+} cell number in
610 chronically infected wildtype and ST2$^{-/-}$ mice (n=3-4 per group, data was pooled from 5
611 experiments and analyzed by randomized block ANOVA)
612 (E) Representative immunofluorescence staining in brain inflammatory foci for iNOS (green)
613 between wildtype and ST2$^{-/-}$ mice, DAPI was used to detect nuclei (blue), scale bar = 50µm
614 (F) Quantification of (E) by iNOS foci voxels in sagittal brain sections of wildtype and ST2$^{-/-}$
615 infected mice using Imaris software, (n=4-5 per group, each data point represents an average of
616 3 sagittal sections, data was pooled from 2 experiments and analyzed by randomized block
617 ANOVA) ns=p>0.05, *=p<0.05, **=p<0.01, ***=p<0.001
618 See also Figure S4.
619
620
621
622
623
624
625

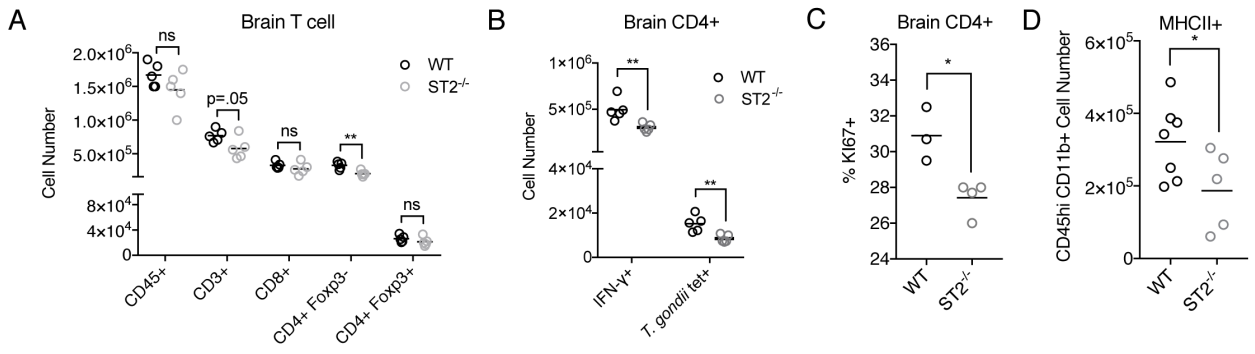

Figure 5. ST2$^{-/-}$ mice have deficient CD4^{+} T cell responses

(A) Flow cytometry measurement of T cell subsets, including total CD45^{+} immune cells, total CD3^{+} T cells, CD8^{+} T cells, CD4^{+} Foxp3^{-} effectors, and CD4^{+} Foxp3^{+} regulatory T cells from chronically infected wildtype and ST2$^{-/-}$ brains (n=5 per group, Student's t-test, representative of 5 independent experiments)

(B) Flow cytometry measurement of activated CD4^{+} T cells which were producing IFN-γ or were specific for a *T. gondii*-MHCII tetramer from chronically infected mice. Wildtype and ST2$^{-/-}$ brain mononuclear cells were stimulated with PMA/ionomycin for 5h (n=5 per group, Student's t-test, representative of 5 independent experiments)

(C) Flow cytometry measurement of Ki67^{+} frequency of brain CD4^{+} T cells from chronically infected wildtype and ST2$^{-/-}$ mice (n=3-4 mice per group, Student's t-test, performed once)

(D) Flow cytometry measurement of brain-infiltrating CD45^{hi} CD11b^{+} MHCII^{+} myeloid cell number in chronically infected wildtype and ST2$^{-/-}$ brains (n=3-4 per group, data was pooled from 2 experiments and analyzed by randomized block ANOVA)

ns=p>0.05, *=p<0.05, **=p<0.01, ***=p<0.001

See also Figure S5.

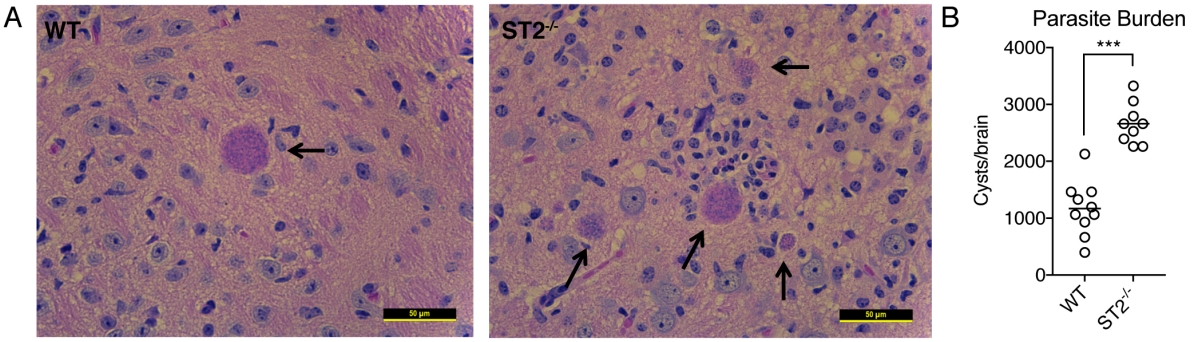

Figure 6. IL-33-ST2 signaling is required for control of brain parasite burden

(A) Hematoxylin and eosin staining of chronically infected brain tissue of wildtype and ST2$^{-/-}$ mice, arrows denote cysts, scale bar = 50μm

(B) Quantification of parasite burden by brain homogenate counts (n=3-4 per group, data was pooled from 3 experiments and analyzed by randomized block ANOVA) ns=p>0.05, *=p<0.05, **=p<0.01, ***=p<0.001

656 **METHODS**

657

658 **Contact for reagent and resource sharing**

659 Further information and requests for resources and reagents should be directed to and will be

660 fulfilled by the Lead Contact, Tajie Harris (tajieharris@virginia.edu).

661

662 **Experimental model and subject details**

663 C57BL/6, CCL2-RFP^{flox}, CCR2^{RFP}, Ai6, and CX3CR1-CreERT2 mice were purchased from

664 Jackson Laboratories. B6.SJL-Ptprc^{a} Pepc^{b}/BoyCrCl (C57BL/6 Ly5.1) mice were purchased from

665 Charles River. ST2$^{-/-}$ mice were generously provided by Andrew McKenzie (Cambridge

666 University). Ordering information for all strains is listed in the key resources table. Animals were

667 housed in a UVA specific pathogen-free facility with a 12h light/dark cycle. Mice were age and

668 sex matched for each experiment and were sacrificed in parallel. Animals were infected with *T.*

669 *gondii* at 7 to 9 weeks of age and were housed separately from breeding animals. All procedures

670 adhered to regulations of the Institutional Animal Care and Use Committee (ACUC) at the

671 University of Virginia.

672

673 **Human Brain tissue**

674 Healthy and toxoplasmic encephalitis human brain samples from adult patients were obtained

675 from the UVA Human Biorepository and Tissue Research Facility. Samples were preserved on

676 paraffin embedded slides. Patient identification and medical background were withheld and

677 therefore IRB approval was not required.

678

679 **Parasite Strains**

680 The avirulent, type II *Toxoplasma gondii* strain Me49 was used for all infections. *T. gondii* cysts

681 were maintained in chronically infected (1-6 months) Swiss Webster (Charles River) mice. To

682 generate cysts for experimental infections, CBA/J (Jackson Laboratories) mice were infected with

683 10 cysts from brain homogenate of Swiss Webster mice by i.p. injection in 200µl PBS. Cysts from
684 4 week-infected CBA/J brain homogenate were then used to infect animals in all experiments.
685
686 **Immunohistochemistry**
687 Mouse Tissue Immunofluorescence:
688 Reporter mice were perfused with 30 mL PBS followed by 30 mL 4% PFA (Electron Microscopy
689 Sciences). All non-reporter strains were not perfused with PFA. Brains were cut along the midline
690 and post-fixed in 4% PFA for 24h at 4°C. Brains were then cryoprotected in 30% sucrose (Sigma)
691 for 24h at 4°C, embedded in OCT (Tissue Tek), and frozen on dry ice. Samples were then stored
692 at -20°C. 40 µm sections were cut using a CM 1950 cryostat (Leica) and placed into a 24-well
693 plate containing PBS. Sections were blocked in PBS containing 2% goat or donkey serum
694 (Jackson ImmunoResearch), 0.1% triton, 0.05% Tween 20, and 1% BSA for 1h at RT. Sections
695 were then incubated with primary antibody diluted in blocking buffer at 4°C overnight. Sections
696 were washed the following day and incubated with secondary antibody in blocking buffer at room
697 temperature for 1h. Sections were then washed and incubated with DAPI (Thermo Scientific) for
698 5 min at RT. Sections were then mounted onto Superfrost microscope slides (Fisherbrand) with
699 aquamount (Lerner Laboratories) and coverslipped (Fisherbrand). Slides were stored at 4°C
700 before use. Images were captured using an TCS SP8 confocal microscope (Leica) and analyzed
701 using Imaris (Bitplane) software. Volumetric analysis was achieved using the surfaces feature of
702 Imaris.
703
704 Human tissue Immunofluorescence:
705 Slides containing 4 µm sections of human brain tissue were received from the UVA Biorepository
706 and Tissue Research Facility and de-paraffinized in a gradient from 100% xylene (Fisher) to 50%
707 ethanol (Decon Laboratories). Slides were then washed in running water and distilled water.

708 Antigen retrieval was performed by incubating slides in antigen retrieval buffer (10 mM sodium
709 citrate, .05%Tween-20, pH 6.0) in an Aroma digital rice cooker for 45 min at 95°C. Slides were
710 then washed in running water followed by PBS-TW. Slides were then incubated with primary and
711 secondary antibodies as described above for mouse brain tissue. Prior to imaging,
712 Autoflourescence Eliminator Reagent was applied per the manufacturer's instructions (EMD
713 Millipore).
714
715 Hematoxylin and Eosin Staining:
716 Brain tissue was fixed in 10% formalin and hematoxylin and eosin staining was performed by the
717 UVA Research Histology Core. Images were acquired on a Brightfield DM 2000 LED microscope
718 (Leica).
719
720 **Tissue processing and flow cytometry**
721 PBS-perfused whole brains were collected in 4 mL of complete RPMI (cRPMI)(10% fetal bovine
722 serum, 1% NEAA, 1% pen/strep, 1% sodium pyruvate, 0.1% β-mercaptoethanol). Papain
723 digestion was performed for the chimera experiment. To perform papain digestion, brains were
724 cut into 6 pieces and incubated in 5 mL HBSS containing 50U/mL DNase (Roche), and 4U/mL
725 papain (Worthington-Biochem) for 45 min at 37°C. Tissue was triturated first with a large bore
726 glass pipette tip, and twice with a small-bore pipette tip every 15 min. In all other experiments
727 collagenase/dispase was used to digest brain tissue. To perform collagenase/dispase digestion,
728 perfused brains were minced using a razor blade and passed through an 18-gauge needle. Brains
729 were then digested with 0.227mg/mL collagenase/dispase and 50U/mL DNase (Roche) for 1h at
730 37°C. Following digestion, homogenate was strained through a 70 µm nylon filter (Corning).
731 Samples were then pelleted and spun in 20 mL 40% Percoll at 650g for 25 min. Myelin was
732 aspirated and cell pellets were washed with cRPMI. Finally, cells were resuspended in cRPMI

733 and cells were enumerated. Spleens were collected into 4 mL cRPMI and macerated through a
734 40 µM nylon filter (Corning). Samples were pelleted and resuspended in 2 mL RBC lysis buffer
735 (0.16 M NH_4Cl) Samples were then washed with cRPMI and resuspended for counting and
736 staining. In cases of acute infection, 4mL of peritoneal lavage fluid was pelleted and resuspended
737 in 2mL of cRPMI for counting and staining. Single cell suspensions were pipetted into a 96 well
738 plate and pelleted. Samples were resuspended in 50 µL Fc Block (1 µg/ml 2.4G2 Ab (BioXCell),
739 0.1% rat gamma globulin (Jackson Immunoresearch)) for 10 min. Cells were then surface stained
740 in 50 µL FACS buffer (PBS, 0.2% BSA, and 2 mM EDTA) for 30 min at 4°C. Following surface
741 staining, cells were fixed for at least 30 min at 4°C with a fixation/permeabilization kit
742 (eBioscience) and permeabilized (eBioscience). Samples were then incubated with intracellular
743 antibodies in permeabilization buffer for 30 min at 4°C. Samples were run on a Gallios flow
744 cytometer (Beckman Coulter), and analyzed using Flowjo software, v. 10.
745
746 **qRT-PCR**
747 Perfused brain tissue (100 mg) was placed into bead beating tubes (Sarstedt) containing 1mL
748 Trizol reagent (Ambion) and zirconia/silica beads (Biospec). Tissue was homogenized for 30
749 seconds with a Mini-bead beater (Biospec) machine. RNA was extracted following
750 homogenization per the Trizol Reagent manufacturer's instructions. Complementary DNA was
751 then synthesized using a High Capacity Reverse Transcription Kit (Applied Biosystems). Taqman
752 gene expression assays were acquired from Applied Biosystems and are listed in the key
753 resources table. A 2X Taq-based mastermix (Bioline) was used for all reactions and run on a
754 CFX384 Real-Time System (Bio-Rad). *Hprt* was used as the brain housekeeping gene and
755 relative expression to wildtype controls was calculated as $2^{(-\Delta\Delta CT)}$.
756
757 ***T. gondii* cyst counts**

758 Brain tissue (100 mg) was minced with a razor in 2mL cRPMI. Brain tissue was then passed
759 through an 18-gauge and 22-gauge needle. 30 μL of resulting homogenate was pipetted onto a
760 microscope slide (VWR) and counted on a Brightfield DM 2000 LED microscope (Leica). Cyst
761 counts were extrapolated for whole brains.
762
763 **Bone marrow chimera**
764 Wildtype B6.SJL-Ptprc^{a} Pepc^{b}/BoyJ (C57BL/6 CD45.1) and ST2KO C57BL/6 mice were irradiated
765 with 1000 rad. Irradiated mice received $3x10^{6}$ bone marrow cells from CD45.1 and CD45.2
766 donors the same day. Bone marrow was transferred by retro-orbital i.v. injection under isoflurane
767 anesthetization. All mice received sulfa-antibiotic water for 2 weeks post-irradiation and were
768 given 6 weeks for bone marrow to reconstitute. At 6 weeks, tail blood was collected from
769 representative mice and assessed for reconstitution by flow cytometry. Mice were then infected
770 for 4 weeks prior to analysis.
771
772 **Statistical analyses**
773 Statistical analyses comparing two groups at one time point were done using a Student's t-test in
774 Prism software, v. 7.0a. In instances where data from multiple infections were combined to
775 illustrate natural variation in virulence, a randomized block ANOVA was performed using R v.
776 3.4.4 statistical software to account for variability across experimental days. Genotype was
777 modeled as a fixed effect and experimental day as a random effect. P values are indicated as
778 follows: ns=not significant $p>.05$, * $p < .05$, ** $p < .01$, *** $p < .001$. The number of mice per group,
779 test used, and p values are denoted in each figure legend. Data was graphed using Prism
780 software, v.7.0a.
781

782 **SUPPLEMENTARY FIGURES**

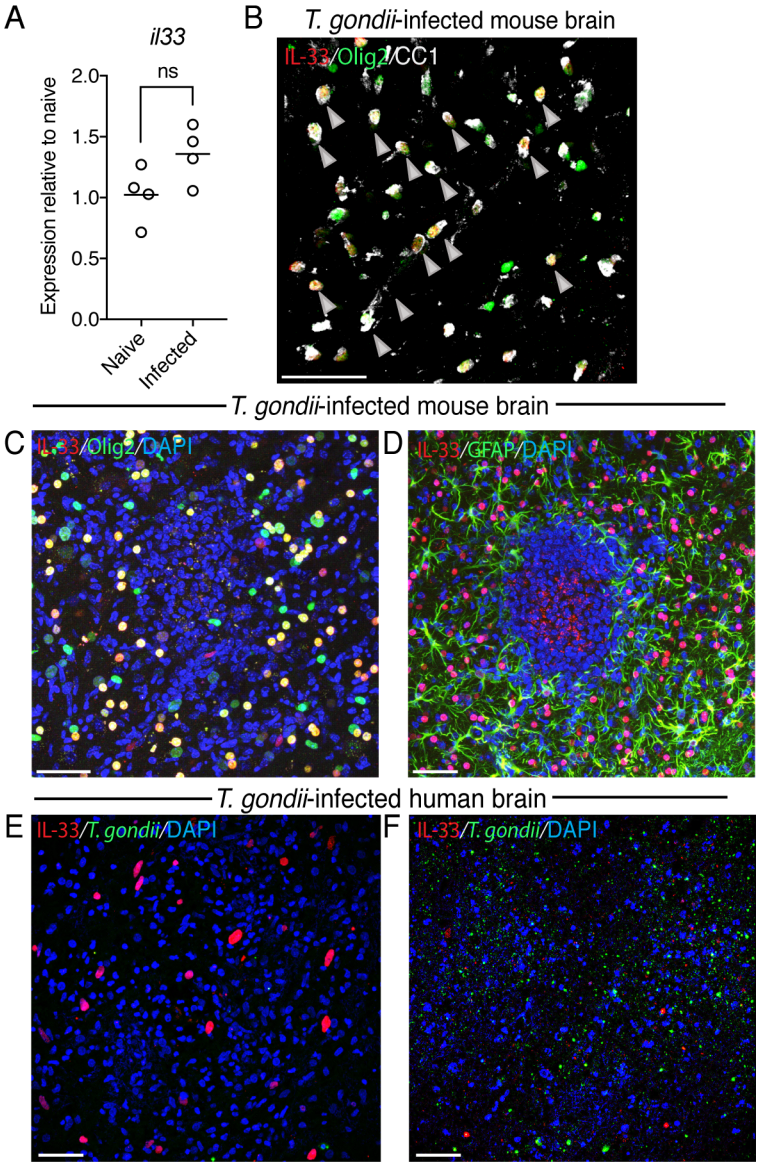

783

784 **Figure S1. IL-33 expression during *T. gondii* infection of mouse and human brain tissue**

785

786 (A) Quantitative real time PCR performed on whole brain homogenate of naïve and chronically

787 infected wildtype mice for detection of *il33* transcript, (n=4 per group, Student's t-test, performed once)

788 (B) Immunofluorescence staining for IL-33 (red), Olig2^{+} oligodendrocytes (green), and CC1^{+} mature

789 oligodendrocyte marker (white) in brain tissue of chronically infected wildtype mice. Gray arrows

790 denote co-localized CC1^{+} Olig2^{+} IL-33^{+} cells

791 (C-D) Representative images of loss of Olig2^{+} oligodendrocytes (C) and GFAP^{+} astrocytes (D) in
792 inflammatory brain regions of chronically infected wildtype mice. Tissue sections were stained for IL-
793 33 (red), Olig2 (green) (C), or IL-33 (red), GFAP^{+} (green) (D) – DAPI was used to visualize nuclei
794 (blue)
795 (E-F) Immunofluorescence staining of *T. gondii* infected human frontal cortex for intact IL-33 (red) in
796 healthier-appearing regions with no *T. gondii* deposition (green) (E), and regions where *T. gondii* was
797 present (F), scale bars = 50μm, ns=p>0.05, *=p<0.05, **=p<0.01, ***=p<0.001
798

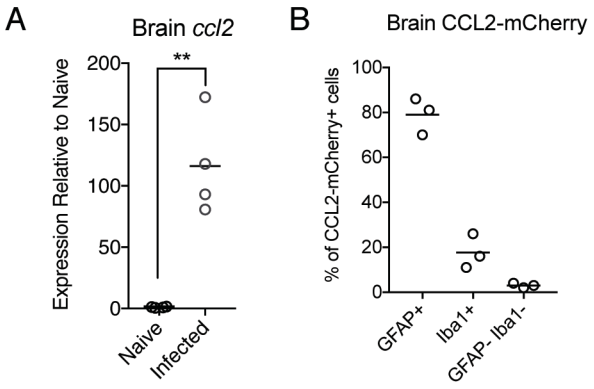

Figure S2. Characterization of brain CCL2 expression during *T. gondii* infection

(A) Quantitative real time PCR performed on whole brain homogenate of naïve and chronically infected wildtype mice for detection of *ccl2* transcript, (n=4 per group, Student's t-test, performed once) (B) Quantification of CCL2-mCherry^{+} cells by percentage of GFAP^{+} astrocytes, Iba1^{+} macrophages, and GFAP^{-} Iba1^{-} cells, (n=3 per group, data points represent an average percentage from approximately 300 cells per mouse, representative of 3 independent experiments)

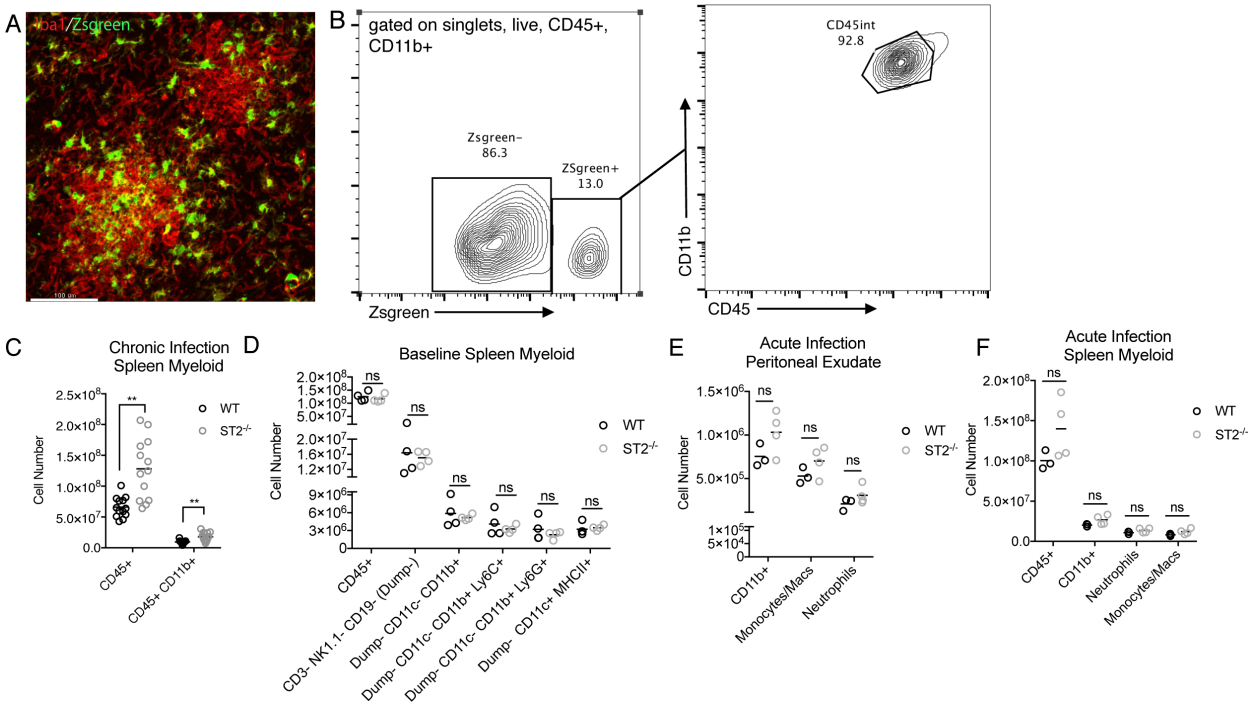

Figure S3. Microglia reporter mice and peripheral myeloid cell responses to infection

(A) Immunofluorescence of inflammatory foci in an infected CX3CR1-creERT2 x Ai6 (ZsGreen cre reporter) mouse – microglia are co-labeled by Zsgreen fluorescence and the macrophage marker Iba1 (red), and peripherally-derived macrophages are Iba1^{+} Zsgreen^{-} scale bar = 100µm

(B) Frequency of Zsgreen^{+} microglia which remain CD45^{int} during chronic infection in a wildtype mouse by flow cytometry

(C) Flow cytometry measurement of CD45^{+} CD11b^{+} cells from chronically infected wildtype and ST2$^{-/-}$ spleens (n=3-4 per group, data was pooled from 5 experiments analyzed by randomized block ANOVA)

(D) Flow cytometry measurement of myeloid cell subsets in uninfected wildtype and ST2$^{-/-}$ spleens (n=4 per group, Student's t-test, representative of 2 independent experiments)

(E) Flow cytometry measurement of total CD11b^{+} myeloid cells, Ly6C^{+} monocytes and macrophages, and Ly6G^{+} neutrophils from peritoneal lavage fluid of wildtype and ST2$^{-/-}$ mice infected for 9 days, n=3-4 per group, Student's t-test, representative of 2 independent experiments)

823 (F) Flow cytometry measurement of total $CD45^+$ immune cells, total $CD11b^+$ myeloid cells, $Ly6C^+$

824 monocytes and macrophages, and $Ly6G^+$ neutrophils from spleens of acutely infected (9 days)

825 wildtype and $ST2^{-/-}$ mice, n=3-4 per group, Student's t-test, representative of 2 independent

826 experiments) ns=p>0.05, *=p<0.05, **=p<0.01, ***=p<0.001

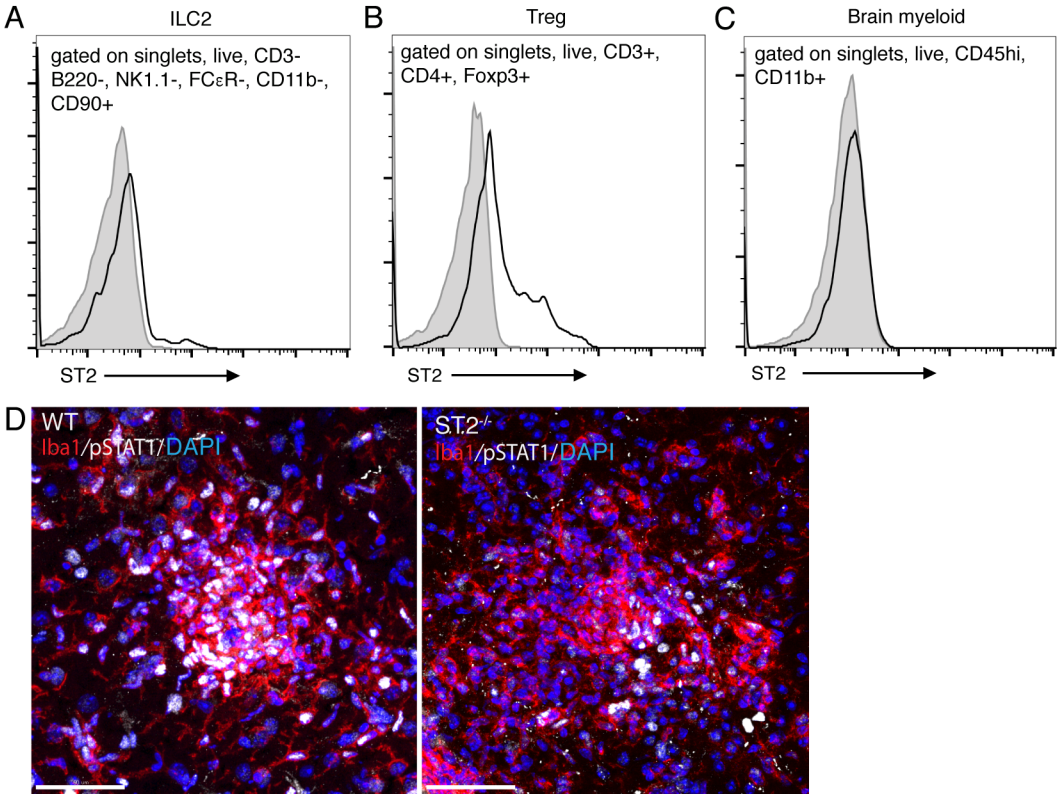

Figure S4. ST2 expression and phosphorylated-STAT1 levels in the CNS during chronic *T. gondii* infection

(A-B) Representative flow cytometry histograms demonstrating ST2 expression on type 2 innate lymphoid cells (A) and regulatory T cells (B) from brains of chronically infected wildtype mice (n=2, representative of 2 independent experiments)

(C) Representative flow cytometry histograms demonstrating lack of ST2 expression on $CD45^{hi}$ $CD11b^{+}$ infiltrating myeloid cells derived from brains of wildtype chronically infected mice, (n=2, representative of 2 independent experiments)

(D) Representative immunofluorescence of inflammatory foci in brains of chronically infected wildtype and $ST2^{-/-}$ mice, stained for $Iba1^{+}$ clustered macrophages (red) and pSTAT1 (white), DAPI was used to detect nuclei (blue), scale bar = 50 μm

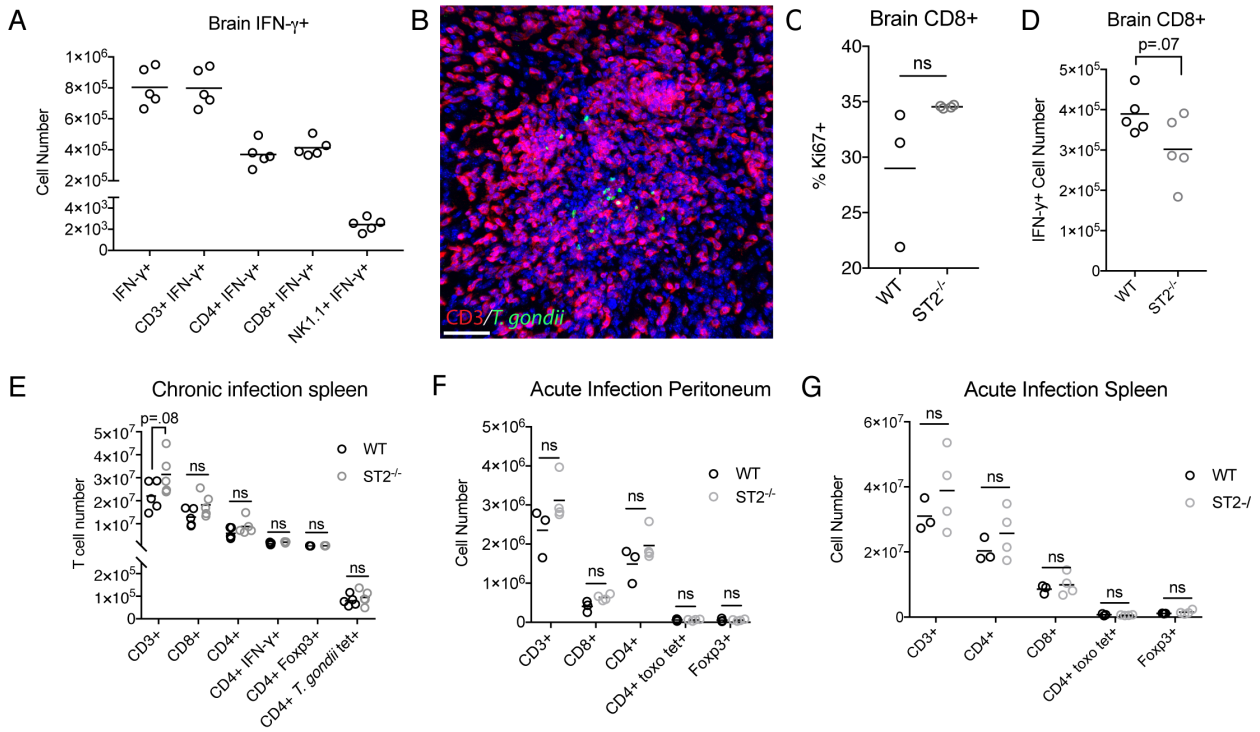

Figure S5. Characterization of T cell responses in wildtype and ST2$^{-/-}$ mice during acute and chronic *T. gondii* infection

(A) Flow cytometry measurement of IFN-γ^{+} CD3^{+} T cells and NK1.1^{+} NK cells from chronically infected brains of wildtype and ST2$^{-/-}$ mice, (n=5 per group, CD3 subsets are representative of 3 independent experiments, and NK cell subset was performed once)

(B) Immunofluorescence staining of reactivated *T. gondii* (green) surrounded by CD3^{+} T cells (red) from a brain of a chronically infected wildtype mouse, scale bar = 50µm

(C) Flow cytometry measurement of Ki67^{+} frequency of brain CD8^{+} T cells from chronically infected wildtype and ST2$^{-/-}$ mice (n=3-4 mice per group, Student's t-test, performed once)

(D) Flow cytometry measurement of CD8^{+} IFN-γ^{+} cell number from brains of chronically infected wildtype and ST2$^{-/-}$ mice, (n=3-4 per group, Student's t-test, representative of 3 independent experiments)

857 (E) Flow cytometry measurement of $CD3^+$ T cell subsets from chronically infected wildtype and
858 $ST2^{-/-}$ spleens (n=5 per group, Student's t-test, representative of 3 independent experiments)
859 (F) Flow cytometry measurement of $CD3^+$ T cell subsets from peritoneal lavage fluid of wildtype
860 and $ST2^{-/-}$ mice infected for 9 days, (n=3-4 per group, Student's t-test, representative of 2
861 independent experiments)
862 (G) Flow cytometry measurement of $CD3^+$ T cell subsets from acutely infected (9 days) wildtype
863 and $ST2^{-/-}$ spleens, (n=3-4 per group, Student's t-test, representative of 2 independent
864 experiments) ns=p>0.05, *=p<0.05, **=p<0.01, ***=p<0.001
865
866